

# Selective Gold-Nanoparticle-Based “Turn-On” Fluorescent Sensors for Detection of Mercury(II) in Aqueous Solution

Chih-Ching Huang<sup>†</sup> and Huan-Tsung Chang<sup>\*†‡</sup>

Department of Chemistry, National Taiwan University, Taipei, Taiwan, and Department of Natural Science Education, National Taitung University, Taitung, Taiwan

A new gold-nanoparticle (AuNP)-based sensor for detecting Hg(II) ions in aqueous solution has been developed. Rhodamine B (RB) molecules that are highly fluorescent in bulk solution fluoresce weakly when they are adsorbed onto AuNP surfaces as a result of fluorescence resonance energy transfer and collision with AuNPs. In the presence of metal ions such as Hg(II), RB molecules are released from the AuNP surface and thus restore the fluorescence of RB. The modulation of the photoluminescence quenching efficiency of RB–AuNPs in the presence of Hg(II) ions can achieve a large turn-on fluorescence enhancement (400-fold) in aqueous solution, and the entire detection takes less than 10 min. We have improved the selectivity of the probe further by modifying the AuNP surfaces with thiol ligands (mercaptosuccinic acid, mercaptosuccinic acid, and homocystine) and adding a chelating ligand (2,6-pyridinedicarboxylic acid) to the sample solutions. Under the optimum conditions, the selectivity of this system for Hg(II) over other metal ions in aqueous solutions is remarkably high (50-fold or more), and its LOD for Hg(II) in the matrix pond water is 2.0 ppb. Our approach demonstrated the feasibility of using the developed nanosensor for rapid determination of Hg(II) in aqueous environmental samples and in batteries.

Heavy metal pollutants exert adverse effects on the environment and also on human health.<sup>1</sup> Environmentally, mercury contamination of ecosystems occurs through a variety of natural and anthropogenic sources, including oceanic and volcanic emissions, gold mining, solid waste incineration, and the combustion of fossil fuels.<sup>2</sup> Physiologically, metallic mercury vapors and organic mercury derivatives (e.g., methylmercury) affect many different areas of the brain and their associated functions, resulting

in symptoms such as personality changes (irritability, shyness, nervousness), tremors, vision problems (constriction or narrowing of the visual field), deafness, and losses of muscle coordination, sensation, and memory.<sup>3</sup> In addition to the brain, inorganic mercury can damage the heart, kidney, stomach, and intestines.<sup>4</sup>

Concerns over toxic exposure to mercury have motivated the exploration of new methods for monitoring aqueous Hg(II). Many current techniques for mercury screening—such as atomic absorption/emission spectroscopy, inductively coupled plasma mass spectrometry (ICPMS), and selective cold vapor atomic fluorescence spectrometry—require expensive and sophisticated instrumentation and/or complicated sample preparation processes.<sup>5</sup> Fluorescence detection with Hg(II)-responsive chemosensors offers a promising approach for simple and rapid tracking of mercury ions in biological, toxicological, and environmental samples.<sup>6,7</sup> Although some fluorescent chemosensors for Hg(II) have been reported (i.e., using small molecules,<sup>6</sup> DNAzymes,<sup>7a</sup> oligonucleotide platforms,<sup>7b</sup> and polymer–protein complexes<sup>7c</sup>), many of these systems exhibit features that limit their practical use, such as poor aqueous solubility, cross-sensitivity toward other metal ions, short emission wavelengths, and/or weak fluorescence intensities. Thus, the development of new, practical assays for Hg(II) remains a challenge.

\* To whom correspondence should be addressed. Phone and fax: 011-886-2-33661171. E-mail: changht@ntu.edu.tw.

<sup>†</sup> National Taiwan University.

<sup>‡</sup> National Taitung University.

- (1) (a) Stern, A. H. *Environ. Res.* **2005**, *98*, 133–142. (b) Zahir, F.; Rizwi, S. J.; Haq, S. K.; Khan, R. H. *Environ. Toxicol. Pharmacol.* **2005**, *20*, 351–360. (c) Campbell, L. M.; Dixon, D. G.; Hecky, R. E. *J. Toxicol. Environ. Health, B* **2003**, *6*, 325–356. (d) Morel, F. M. M.; Kraepiel, A. M. L.; Amyot, M. *Annu. Rev. Ecol. Syst.* **1998**, *29*, 543–566.
- (2) (a) Wang, Q.; Kim, D.; Dionysiou, D. D.; Sorial, G. A.; Timberlake, D. *Environ. Pollut.* **2004**, *131*, 323–336. (b) Tchounwou, P. B.; Ayensu, W. K.; Ninashvili, N.; Sutton, D. *Environ. Toxicol.* **2003**, *18*, 149–175. (c) Eisler, R. *Environ. Geochem. Health* **2003**, *25*, 325–345.

- (3) (a) Mutter, J.; Naumann, J.; Schneider, R.; Walach, H.; Haley, B. *Neuroendocrinol. Lett.* **2005**, *26*, 439–446. (b) Zheng, W.; Aschner, M.; Ghersi-Egea, J.-F. *Toxicol. Appl. Pharmacol.* **2003**, *192*, 1–11.
- (4) (a) Hoyle, I.; Handy, R. D. *Aquat. Toxicol.* **2005**, *72*, 147–159. (b) Zalups, R. K. *Pharmacol. Rev.* **2000**, *52*, 113–143. (c) Kobal, A. B.; Horvat, M.; Prezelj, M.; Briški, A. S.; Krsnik, M.; Dizdarević, T.; Mazej, D.; Fahnoga, I.; Stibilj, V.; Arnerič, N.; Kobal, D.; Osredkar, J. *J. Trace Elem. Med. Biol.* **2004**, *17*, 261–274. (d) Vupputuri, S.; Longnecker, M. P.; Daniels, J. L.; Guo, X.; Sandler, D. P. *Environ. Res.* **2005**, *97*, 194–199. (e) Baughman, T. A. *Environ. Health Perspect.* **2006**, *114*, 147–152.
- (5) (a) Butler, O. T.; Cook, J. M.; Harrington, C. F.; Hill, S. J.; Rieuwert, J.; Miles, D. L. *J. Anal. At. Spectrom.* **2006**, *21*, 217–243. (b) Li, Y.; Chen, C.; Li, B.; Sun, J.; Wang, J.; Gao, Y.; Zhao, Y.; Chai, Z. *J. Anal. At. Spectrom.* **2006**, *21*, 94–96. (c) Leermakers, M.; Baeyens, W.; Quevauviller, P.; Horvat, M. *Trends Anal. Chem.* **2005**, *24*, 383–393.
- (6) (a) Nolan, E. M.; Lippard, S. J. *J. Am. Chem. Soc.* **2003**, *125*, 14270–14271. (b) Yang, Y.-K.; Yook, K.-J.; Tae, J. *J. Am. Chem. Soc.* **2005**, *127*, 16760–16761. (c) Yoon, S.; Albers, A. E.; Wong, A. P.; Chang, C. J. *J. Am. Chem. Soc.* **2005**, *127*, 16030–16301. (d) Moon, S.-Y.; Youn, N. J.; Park, S. M.; Chang, S.-K. *J. Org. Chem.* **2005**, *70*, 2394–2397. (e) Nolan, E. M.; Racine, M. E.; Lippard, S. J. *Inorg. Chem.* **2006**, *45*, 2742–2749.
- (7) (a) Thomas, J. M.; Ting, R.; Perrin, D. M. *Org. Biomol. Chem.* **2004**, *2*, 307–312. (b) Ono, A.; Togashi, H. *Angew. Chem., Int. Ed.* **2004**, *43*, 4300–4302. (c) Kim, I.-B.; Bunz, U. H. F. *J. Am. Chem. Soc.* **2006**, *128*, 2818–2819.

One potential approach is the use of nanoparticles (NPs), which provide high sensitivity for the detection of metal ions because their optical properties exhibit strong size, shape, and interparticle distance dependences.<sup>8</sup> Recently, a simple and selective approach was reported for the determination of Hg(II) in tap water using a gold nanorod solution in the presence of sodium borohydride.<sup>8i</sup> The approach provides a limit of detection (LOD)—at a signal-to-noise (S/N) ratio of 3—for Hg(II) on the parts-per-trillion level with good precision and accuracy. On the basis of our experience, several other metal ions such as silver, iron, and copper also induce the change in the surface plasmon resonance (SPR) extinction of gold nanorods, which may interfere with the analysis of Hg(II).<sup>9</sup> Another related example is a homogeneous assay that used gold NPs (AuNPs) to detect Cu(II) on the basis of its modulation of the photoluminescence quenching efficiency between a perylene bisimide chromophore and AuNPs.<sup>8a</sup> When fluorophore-containing pyridyl moieties are coordinated to AuNPs through weak N–Au interactions, fluorescence quenching occurs by AuNPs that are ultraefficient quenchers. Owing to a stronger coordination of the pyridyl moiety to Cu(II) ion than to the AuNPs, the fluorescence of the fluorophore is turned on when it binds to the Cu(II). The sensor provides the detection limit of 1.0  $\mu\text{M}$  for Cu(II) and 2–3-fold selectivity against other metal ions. One disadvantage of this approach is that the sensor works well only in the organic phase.

AuNPs are unique quenchers for chromophores through both energy-transfer and electron-transfer processes.<sup>10</sup> AuNPs have a Stern–Volmer quenching constant ( $K_{\text{SV}}$ ) that is several orders of magnitude greater than that of typical small molecule dye–quencher pairs. This superquenching property of AuNPs allows them to be employed as effective proximal quenchers in optical detection of DNA through hybridization with complementary-DNA-modified AuNPs and of antigens through highly specific affinity with antibody-modified AuNPs.<sup>11,12</sup> Although many ap-

plications of AuNPs in bioanalyses of large molecules and organic molecules have been demonstrated, very few studies have been carried out for highly selective and sensitive detection of heavy metal ions in aqueous solution by taking advantage of photoluminescent quenching of AuNPs.

The aim of this study is to develop a highly sensitive and selective AuNP-based nanosensor for the determination of Hg(II) in aqueous solution. We prepared Rhodamine B (RB)–AuNP (RB–AuNP) via RB self-adsorbed on the surface of AuNPs.<sup>13</sup> The fluorescence of RB switched to turn-on upon addition of Hg(II). By modification of AuNPs with thiol ligands, such as mercaptopropionic acid (MPA), and adding a chelating ligand, 2,6-pyridinedicarboxylic acid (PDCA), to the solutions, the selectivity toward Hg(II) against other metal ions improved.

## EXPERIMENTAL SECTION

**Chemicals.** MPA, mercaptosuccinic acid (MSA), homocysteine (HCys), PDCA, and RB were obtained from Sigma (St. Louis, MO). Trisodium citrate and all metallic salts used in this study were purchased from Aldrich (Milwaukee, WI). Sodium tetraborate and hydrogen tetrachloroaurate(III) trihydrate were obtained from Acros (Geel, Belgium).

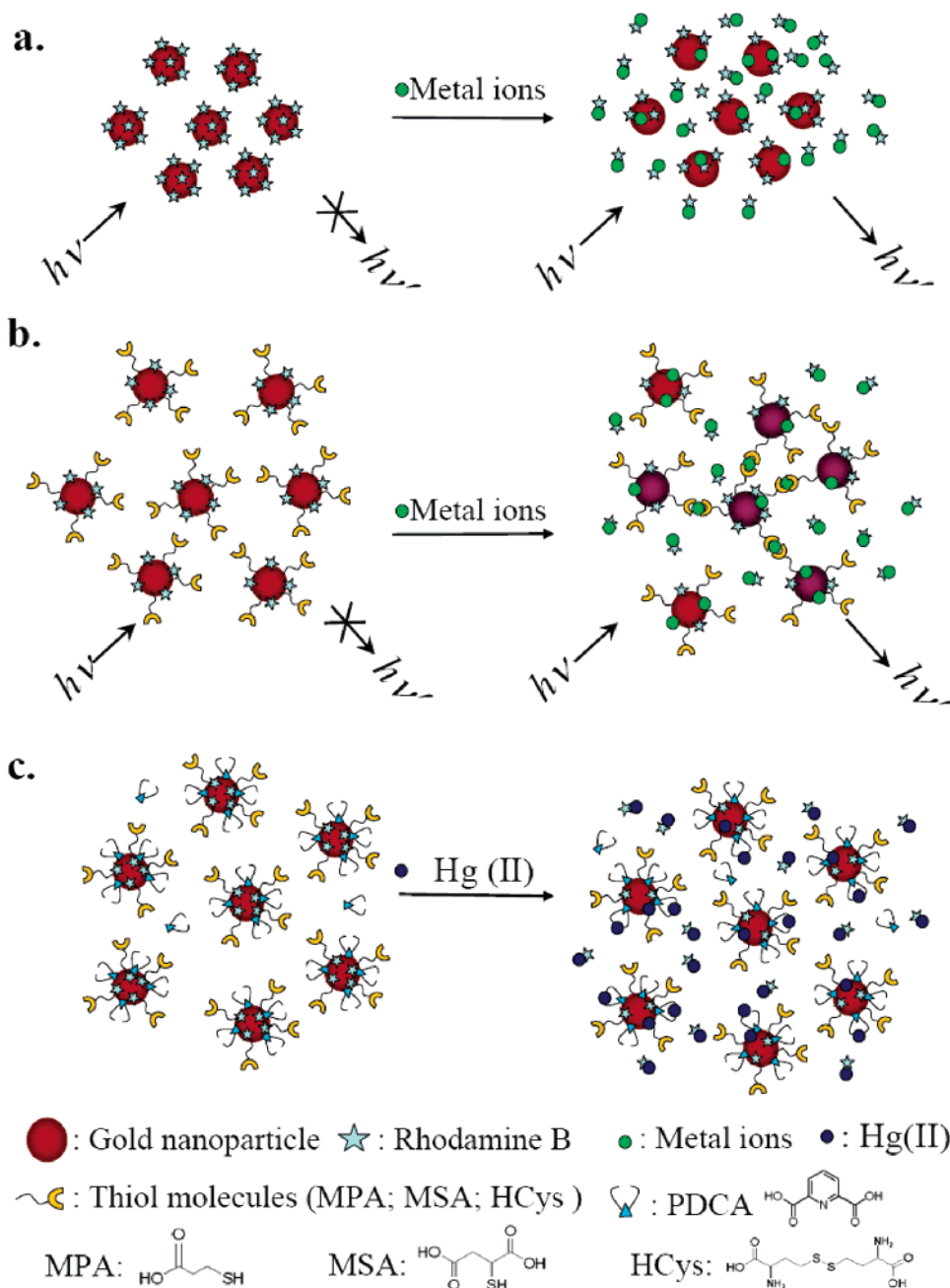
**Synthesis of AuNPs.** AuNPs were prepared by citrate reduction of  $\text{HAuCl}_4$ .<sup>14</sup> A 250 mL aqueous solution consisting of 1 mM  $\text{HAuCl}_4$  was brought to a vigorous boil with stirring in a round-bottom flask fitted with a reflux condenser; 38.8 mM trisodium citrate (25 mL) was then added rapidly to the solution. The solution was heated under reflux for another 15 min, during which time its color changed from pale yellow to deep red. The solution was cooled to room temperature while being stirred continuously. The sizes of the nanoparticles were verified by TEM analysis (H7100, Hitachi High-Technologies Corp., Tokyo, Japan); the AuNPs appeared to be nearly monodisperse, with an average size of  $13.3 \pm 1.2$  nm. The particle concentration of the AuNPs (ca. 15 nM) was determined according to Beer's law using an extinction coefficient of ca.  $10^8 \text{ M}^{-1} \text{ cm}^{-1}$  at 520 nm (double-beam UV–vis spectrophotometer, Cintra 10e, GBC, Victoria, Australia) for AuNPs of 13.3 nm diameter.<sup>14c</sup>

**Modification of AuNPs.** A stock solution of RB (2 mM) was prepared in DI water. An aliquot of RB solution (2 mM, 10  $\mu\text{L}$ ) was added with stirring to a solution of the 13 nm diameter AuNPs (6 nM, 10 mL), which were prepared in 5 mM sodium tetraborate (pH 9.0). The solution was equilibrated at ambient temperature for 2 h. The fluorescence spectrum of the as-prepared RB–AuNP solution was measured using a Hitachi F-4500 fluorescence spectrophotometer with excitation at 510 nm. The very low fluorescence observed in the fluorescence spectrum of the RB–AuNP solution indicated that effectively all of the RB molecules had adsorbed onto the AuNPs and that their fluorescence was strongly quenched by the AuNPs via FRET processes.<sup>10</sup> RB–

- (8) (a) He, X.; Liu, H.; Li, Y.; Wang, S.; Li, Y.; Wang, N.; Xiao, J.; Xu, X.; Zhu, D. *Adv. Mater.* **2005**, *17*, 2811–2815. (b) Kim, Y.; Johnson, R. C.; Hupp, J. T. *Nano Lett.* **2001**, *1*, 165–167. (c) Liu, J.; Lu, Y. *J. Am. Chem. Soc.* **2005**, *127*, 12677–12683. (d) Wanunu, M.; Popovitz-Biro, R.; Cohen, H.; Vaskevich, A.; Rubinstein, I. *J. Am. Chem. Soc.* **2005**, *127*, 9207–9215. (e) Sugunan, A.; Thanachayanont, C.; Dutta, J.; Hilborn, J. G. *Sci. Technol. Adv. Mater.* **2005**, *6*, 335–340. (f) Lin, S.-Y.; Chen, C.-H.; Lin, M.-C.; Hsu, H.-F. *Anal. Chem.* **2005**, *77*, 4281–4288. (g) Norsten, T. B.; Frankamp, B. L.; Rotello, V. M. *Nano Lett.* **2002**, *2*, 1345–1348. (h) Obare, S. O.; Hollowell, R. E.; Murphy, C. J. *Langmuir* **2002**, *18*, 10407–10410. (i) Rex, M.; Hernandez, F. E.; Campiglia, A. D. *Anal. Chem.* **2006**, *78*, 445–451.
- (9) (a) Yang, Z.; Lin, Y.-W.; Tseng, W.-L.; Chang, H.-T. *J. Mater. Chem.* **2005**, *15*, 2450–2454. (b) Huang, C.-C.; Yang, Z.; Chang, H.-T. *Langmuir* **2004**, *20*, 6089–6092. (c) Yang, Z.; Chang, H.-T. *Nanotechnology* **2006**, *17*, 2304–2310. (d) Huang, Y.-F.; Huang, K.-M.; Chang, H.-T. *J. Colloid Interface Sci.* **2006**, *301*, 145–154.
- (10) (a) Kamat, P. V.; Barazzouk, S.; Hotchandani, S. *Angew. Chem., Int. Ed.* **2002**, *41*, 2764–2767. (b) Dulkeith, E.; Morteaux, A. C.; Niedereichholz, T.; Klar, T. A.; Feldmann, J.; Levi, S. A.; van Veggel, F. C. J. M.; Reinhoudt, D. N.; Möller, M.; Gittins, D. I. *Phys. Rev. Lett.* **2002**, *89*, 203002. (c) Huang, T.; Murray, R. W. *Langmuir* **2002**, *18*, 7077–7081. (d) Fan, C.; Wang, S.; Hong, J. W.; Bazan, G. C.; Plaxco, K. W.; Heeger, A. J. *Proc. Natl. Acad. Sci. U.S.A.* **2003**, *100*, 6297–6301.
- (11) (a) Maxwell, D. J.; Taylor, J. R.; Nie, S. *J. Am. Chem. Soc.* **2002**, *124*, 9606–9612. (b) Dubertret, B.; Calame, M.; Libchaber, A. *J. Nat. Biotechnol.* **2001**, *19*, 365–370. (c) Li, H.; Rothberg, L. J. *Anal. Chem.* **2004**, *76*, 5414–5417. (d) Wu, Z.-S.; Jiang, J.-H.; Fu, L.; Shen, G.-L.; Yu, R.-Q. *Anal. Biochem.* **2006**, *353*, 22–29.
- (12) (a) Ao, L.; Gao, F.; Pan, B.; He, R.; Cui, D. *Anal. Chem.* **2006**, *78*, 1104–1106. (b) Kato, N.; Caruso, F. *J. Phys. Chem. B* **2005**, *109*, 19604–19612. (c) Huang, C.-C.; Huang, Y.-F.; Cao, Z.; Tan, W.; Chang, H.-T. *Anal. Chem.* **2005**, *77*, 5735–5741.

- (13) (a) Chen, S.-J.; Chang, H.-T. *Anal. Chem.* **2004**, *76*, 3727–3734. (b) Lim, I.-I. S.; Goroleski, F.; Mott, D.; Kariuki, N.; Ip, W.; Luo, J.; Zhong, C.-J. *J. Phys. Chem. B* **2006**, *110*, 6673–6682. (c) Franzen, S.; Folmer, J. C. W.; Glomm, W. R.; O'Neal, R. J. *Phys. Chem. A* **2002**, *106*, 6533–6540. (d) Fang, J.; Huang, Y.; Li, X.; Dou, X. *J. Raman Spectrosc.* **2004**, *35*, 914–920. (f) Ghosh, S. K.; Pal, A.; Kundu, S.; Nath, S.; Pal, T. *Chem. Phys. Lett.* **2004**, *395*, 366–372.
- (14) (a) Frens, G. *Nat. Phys. Sci.* **1973**, *241*, 20–22. (b) Grabar, K. C.; Freeman, R. G.; Hommer, M. B.; Natan, M. J. *Anal. Chem.* **1995**, *67*, 735–743. (c) Mucic, R. C.; Storhoff, J. J.; Mirkin, C. A.; Letsinger, R. L. *J. Am. Chem. Soc.* **1998**, *120*, 12674–12675.

**Scheme 1. Schematic Representations of Hg(II) Nanosensors That Operate on the Basis of Modulation of the FRET between RB and AuNPs<sup>a</sup>**



<sup>a</sup> Key: (a) RB–AuNP-based sensor; (b) RB–AuNP–thiol-based sensor; (c) PDCA/RB–AuNP–thiol-based sensor;  $h$  = Planck's constant;  $\nu$  = frequency of light.

AuNP–MPA, RB–AuNP–MSA, and RB–AuNP–HCys were prepared by adding 10 mM MPA, MSA, and HCys (10  $\mu$ L), respectively, to individual 13 nm diameter AuNP solutions (15 nM, 10 mL) with stirring. After reaction for 2 h at room temperature, the mixtures were prepared in 5 mM sodium borate at pH 9.0. The final concentrations of AuNP–MPA, AuNP–MSA, and AuNP–HCys were each 6.0 nM. Finally, an aliquot of the RB solution (0.4 mM, 10  $\mu$ L) was added to each of the as-prepared AuNP–MPA, AuNP–MSA, and AuNP–HCys solutions (6 nM, 10 mL). The solutions were equilibrated at ambient temperature for 2 h. The fluorescence spectra of these RB–AuNP–MPA, RB–AuNP–MSA, and RB–AuNP–HCys solutions were recorded to

ensure no excess RB was free in solution. Similarly, very weak fluorescence was observed from these three solutions.

**Analysis of Pond Water and Battery Samples.** A water sample from a pond on our campus was filtered through a 0.2  $\mu$ m membrane and analyzed by ICPMS. Aliquots of the pond water (0.49 mL) were spiked with standard solutions (10  $\mu$ L) containing Hg(II) at concentrations over the range of 0.01–1.0  $\mu$ M. The mixtures were then diluted to 1.0 mL with 0.5 mL of 5 mM tetraborate (pH 9.0) buffer and were analyzed by the present approach using 0.6 nM RB–AuNP–MPA probe solutions. The sample preparation of button-type alkaline manganese batteries for detection of mercury was according to the standard method



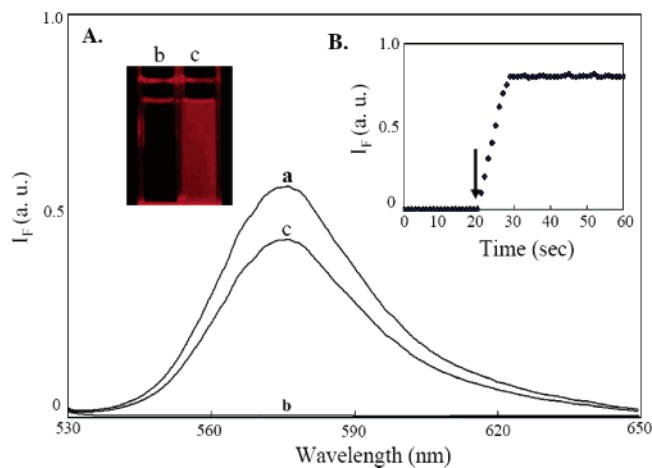


**Figure 1.** Fluorescence spectra of solutions of (a) RB and (b, c) RB–AuNPs in the (b) absence and (c) presence of Hg(II) ( $100 \mu\text{M}$ ). The concentrations of the AuNPs and RB were  $3.0 \text{ nM}$  and  $1.0 \mu\text{M}$ , respectively. Inset A: Fluorescence photographs of RB–AuNPs in the (b) absence and (c) presence of Hg(II) ( $100 \mu\text{M}$ ). Inset B: Time course measurement of fluorescence intensity ( $575 \text{ nm}$ ) for RB–AuNP upon the addition of Hg(II) ( $100 \mu\text{M}$ ). The arrow indicates the initial time of adding Hg(II). Buffer:  $5 \text{ mM}$  sodium tetraborate, pH  $9.0$ . Excitation wavelength:  $510 \text{ nm}$ . The fluorescence intensities ( $I_f$ ) are plotted in arbitrary units (au).

published by the National Electrical Manufacturers Association.<sup>15</sup> Briefly, the battery samples were subjected to digestion in a 2:1 (v/v) mixture of HCl and HNO<sub>3</sub> for 18 h, and the resulting solutions were directly basified by adding  $0.5 \text{ N}$  NaOH and filtered with a  $0.2 \mu\text{m}$  membrane. The solutions ( $10 \mu\text{L}$ ) were then diluted to  $10 \text{ mL}$  with  $5 \text{ mM}$  tetraborate (pH  $9.0$ ) buffer prior to analysis by ICPMS and by the present approach using a  $0.6 \text{ nM}$  RB–AuNP–MPA probe. The quantitation of mercury in the batteries was obtained by standard addition.

## RESULTS AND DISCUSSION

**AuNP-Based Sensor for Hg(II).** As indicated in Scheme 1a, the sensing mechanisms occur through two routes: (i) Hg(II) ions displacing RB dye molecules from the surfaces of AuNPs and (ii) RB departing from the AuNPs as a result of the deposition of Hg<sup>0</sup> through the reduction of Hg(II) ions by citrate on the AuNPs. In their unbound state, RB molecules are highly fluorescent, but when they have been adsorbed noncovalently onto the surfaces of  $13 \text{ nm}$  diameter AuNPs, fluorescence resonance energy transfer (FRET) and collision occur between RB and the AuNPs.<sup>10,13a,e</sup> As a result, the fluorescence of RB is almost completely quenched by the AuNPs, as illustrated in Figure 1. The main reasons why we chose to use RB as the dye in this study are its water solubility, photostability, and high extinction coefficient and quantum yield, as well as its ability to form ion association complexes with Hg(II).<sup>16</sup> As indicated in Figure 1, upon the addition of  $100 \mu\text{M}$  Hg(NO<sub>3</sub>)<sub>2</sub> to a solution of RB–AuNPs (probe), which were prepared in  $5 \text{ mM}$  sodium tetraborate at pH

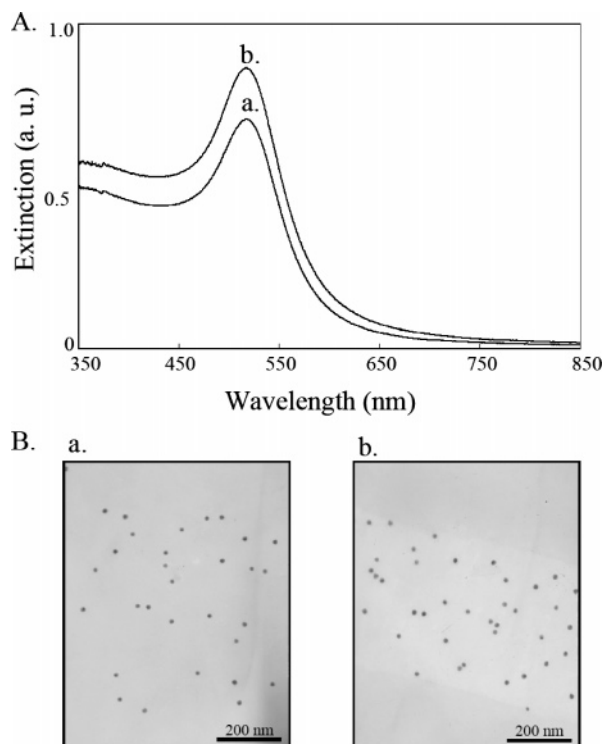


**Figure 2.** (A) UV–vis absorbance spectra and (B) TEM images of solutions containing RB–AuNPs in the (a) absence and (b) presence ( $100 \mu\text{M}$ ) of Hg(II). The concentrations of the AuNPs and RB were  $3.0 \text{ nM}$  and  $1.0 \mu\text{M}$ , respectively. Buffer:  $5 \text{ mM}$  sodium tetraborate solution, pH  $9.0$ . Other conditions were the same as those described for Figure 1.

$9.0$ , the RB units departed from the AuNPs' surfaces, leading to a ca. 400-fold increase in fluorescence. Inset B in Figure 1 suggests that the reaction reached completion within  $10 \text{ s}$ , the time frame of these measurements. In addition, deposition of mercury atoms onto the AuNPs was evidenced by increases in the surface plasmon resonance (SPR) extinction band in the UV–vis absorption spectrum (Figure 2A).<sup>17</sup> There was no statistical difference in the average particle diameter or size distribution increases in the mean size of AuNPs as determined from TEM images (Figure 2B), which is similar to the report that there is only a submonolayer of Hg on the surface of AuNPs.<sup>17a</sup> From related fluorescence, UV–vis absorption, and TEM measurements, we obtained similar results when using other mercury salts, such as HgCl<sub>2</sub> and Hg(ClO<sub>4</sub>)<sub>2</sub> (data not shown); i.e., it appears that the counter anions exert a negligible effect on our probe. As a reference, we did not observe any difference in the fluorescence spectrum of pure RB ( $200 \text{ nM}$ ) after the addition of Hg(II) ( $100 \mu\text{M}$ ).

**Selectivity of the AuNP-Based Sensor.** We also investigated (Figure 3a) the changes in the fluorescence spectra of the RB–AuNPs ( $3 \text{ nM}$ )<sup>18</sup> that occurred within  $5 \text{ min}$  of adding the following metal ions ( $100 \mu\text{M}$ ): Mg(II), Ca(II), Sr(II), Fe(II), Mn(II), Cu(II), Co(II), Ni(II), Zn(II), Pd(II), Pb(II), Cd(II), Al(III), Cr(III),

(15) EPBA, BAT, and NEMA. *Battery Industry standard analytical method for the determination of mercury, cadmium and lead in alkaline manganese cells using AAS, ICP-AES and cold vapor*; European Portable Battery Association (EPBA), Battery Association of Japan (BAT), and National Electrical Manufacturers Association (NEMA): Brussels, Belgium, Tokyo, and Rosslyn, VA, respectively, April 1998.

(16) (a) Vedrına-Dragojević, I.; Dragojević, D.; Čadež, S. *Anal. Chim. Acta* **1997**, *355*, 151–156. (b) Balint, L.; Vedrına-Dragojević, I.; Šebečić, B.; Momirović-Čuljat, J.; Horvatić, M. *Mikrochim. Acta* **1997**, *127*, 61–65. (c) Li, H.-B.; Chen, F.; Xu, X.-R. *Fresenius' J. Anal. Chem.* **2000**, *367*, 499–501. (d) Gao, H. W. *Asian J. Chem.* **2000**, *12*, 78–84.  
(17) (a) Morris, T.; Copeland, H.; McLinden, E.; Wilson, S.; Szulcowski, G. *Langmuir* **2002**, *18*, 7261–7264. (b) Henglein, A.; Giesig, M. *J. Phys. Chem. B* **2000**, *104*, 5056–5060.

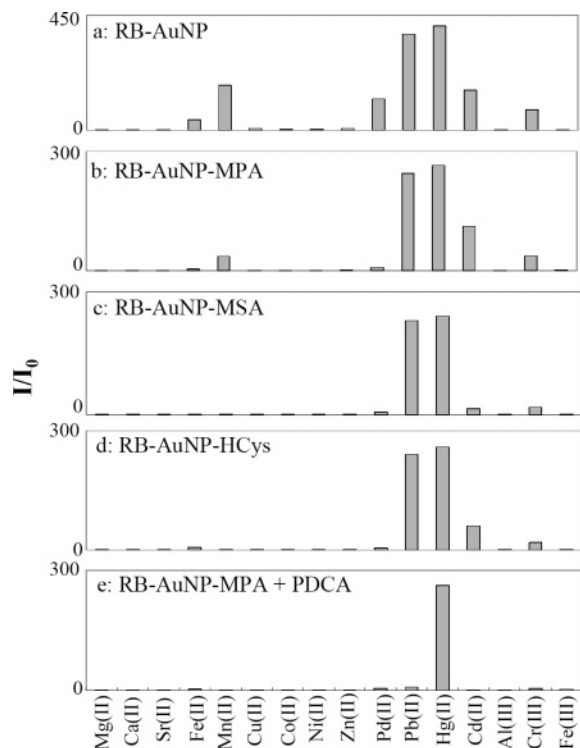


**Figure 3.** Enhanced ratios ( $I/I_0$ ) of the fluorescence intensity (575 nm) of the (a) RB–AuNP, (b) RB–AuNP–MPA, (c) RB–AuNP–MSA, (d) RB–AuNP–HCys, and (e) RB–AuNP–MPA systems in the presence of PDCA (1.0 mM) upon the addition of 100  $\mu$ M metal ions in 5 mM sodium tetraborate at pH 9.0. Other conditions were the same as those described for Figure 1.

and Fe(III). From this series of ions, we found that the presence of Fe(II), Mn(II), Pd(II), Pb(II), Cd(II), and Cr(III) ions led to increases in the fluorescence intensity to varying degrees, whereas the remaining ions exhibited no significant effects under identical conditions. The fluorescence spectra of the supernatants of the mixtures after centrifuging were similar to the original solutions, and in the control experiments all metal ions did not affect or slightly affected the fluorescence spectrum of pure RB. These results mean that the enhanced fluorescence of the solution was due to RB departing from AuNPs by Fe(II), Mn(II), Pd(II), Pb(II), Cd(II), and Cr(III) ions and thus the fluorescence being restored. However, these results (Figure 3a) suggest poor selectivity of the RB–AuNP probe toward Hg(II) with respect to Fe(II), Mn(II), Pd(II), Pb(II), Cd(II), and Cr(III) ions.

To overcome this problem, we modified the AuNP surfaces with ligands that form stable complexes with the interfering metal ions and Hg(II) (Scheme 1b).<sup>8b</sup> MPA, MSA, and HCys were bound to the surfaces of AuNPs through Au–S bonding, leading to the preparation of AuNP–MPA, AuNP–MSA, and AuNP–HCys species, respectively.<sup>19</sup> The coverage areas of these thiol ligands on the surface of AuNPs were all about 20%, which were determined by monitoring the fluorescence increases of RB

molecules when they were displaced from RB–AuNPs by thiols as described in our previous paper.<sup>13a</sup> Addition of the appropriate amounts of RB to these three thiol-modified AuNP solutions allowed preparation of very low background intensity probe solutions of RB–AuNP–MPA, RB–AuNP–MSA, and RB–AuNP–HCys systems, respectively. The RB molecules adsorbed onto the surfaces of the thiol-modified AuNPs and the thiol compounds retained their chelating ability toward heavy metal ions.<sup>8b</sup> As indicated in Scheme 1b, the RB–AuNP–MPA, RB–AuNP–MSA, and RB–AuNP–HCys cross-links aggregated in solution in the presence of some metal ions, such as Pb(II) and Cd(II), driven by heavy metal ion recognition and binding, yielding both a substantial shift in the plasmon band energy to longer wavelength and a red-to-blue color change (data not shown).<sup>8</sup> Parts b–d of Figure 3 illustrate the fluorescence responses of RB–AuNP–MPA, RB–AuNP–MSA, and RB–AuNP–HCys toward the various metal ions. Although RB–AuNP–MPA, RB–AuNP–MSA, and RB–AuNP–HCys exhibited decreased or negligible responses toward Fe(II), Mn(II), and Cr(III), these sensors remained selective for Hg(II), Pb(II), and Cd(II). These results were similar to the reports that suggest RB molecules are capable of forming ion association complexes with Hg(II), Pb(II), and Cd(II).<sup>16,20</sup> It also cannot be excluded that the chelation and aggregation mediated by heavy metal ions such as Pb(II) and Cd(II) may cause RB to depart from the surfaces of AuNPs through a steric effect.<sup>8b</sup>

Fortunately, specificity of the RB–AuNP–MPA, RB–AuNP–MSA, and RB–AuNP–HCys probes toward Hg(II), with respect to the other metal ions, was readily achieved in the presence of 1 mM PDCA (Scheme 1c), which we added at ca. 10 times the concentration of Hg(II) (100  $\mu$ M) to ensure better masking and the formation of stable complexes with Hg(II); PDCA forms much more stable complexes with heavy metal ions such as Hg(II) ( $\log \beta_2 = 20.28$ ) than with other metal ions.<sup>21</sup> As indicated in Figure 3e, RB–AuNP–MPA in 5 mM tetraborate (pH 9.0) containing 1.0 mM PDCA responded with high selectivity (50-fold or more) toward Hg(II) ions with respect to the other metal ions; RB–AuNP–MSA and RB–AuNP–HCys exhibited similar selectivities (Figure S1, Supporting Information). These results suggest that some PDCA ligands were bound to the RB–AuNP–MPA, RB–AuNP–MSA, and RB–AuNP–HCys species, improving their selectivity toward Hg(II), while PDCA ligands in the bulk solutions formed complexes with the other metal ions, suppressing their interference. We also tested the selectivity of the RB–AuNPs toward Hg(II) in the presence of PDCA. In comparison with the thiol-modified RB–AuNPs, the RB–AuNPs provided relatively poor selectivity toward Hg(II) (Figure 4), suggesting that Hg(II) ions most likely form stable complexes with the carboxylic acid units of the surface thiol and PDCA ligands. Thus, we conclude that modification of the AuNP surfaces with thiol ligands is an essential part of increasing the selectivity toward Hg(II).

(18) The concentration refers to that of the AuNPs.

(19) (a) Templeton, A. C.; Wuelfing, W. P.; Murray, R. W. *Acc. Chem. Res.* **2000**, *33*, 27–36. (b) Reynolds, R. A., III; Mirkin, C. A.; Letsinger, R. L. *J. Am. Chem. Soc.* **2000**, *122*, 3795–3796. (c) Cao, Y. W.; Jin, R. C.; Mirkin, C. A. *J. Am. Chem. Soc.* **2001**, *123*, 7961–7962. (d) Kassam, A.; Bremner, G.; Clark, B.; Ulibarri, G.; Lennox, R. B. *J. Am. Chem. Soc.* **2006**, *128*, 3476–3477.

(20) (a) Liu, S.; Liu, Y.; Liu, Z. *Microchim. Acta* **1983**, *81*, 5–6. (b) Das, S. N.; Panda, M. *Asian J. Spectrosc.* **2003**, *7*, 87–92. (c) Shakhverdov, T. A.; Ergashev, R. *Opt. Spectrosc.* **1999**, *87*, 219–224.

(21) (a) Suzuki, K.; Yamasaki, K. *Naturwissenschaften* **1957**, *44*, 396–396. (b) Ahmed, I. T.; El-Roudi, O. M.; Boraei, A. A. A.; Ibrahim, S. A. *J. Chem. Eng. Data* **1996**, *41*, 386–390. (c) Ding, X.-J.; Mou, S.-F.; Liu, K. N.; Siriraks, A.; Riviello, J. *Anal. Chim. Acta* **2000**, *407*, 319–326. (d) Norkus, E.; Stalnionienė, I.; Crans, D. C. *Heterat. Chem.* **2003**, *14*, 625–632.

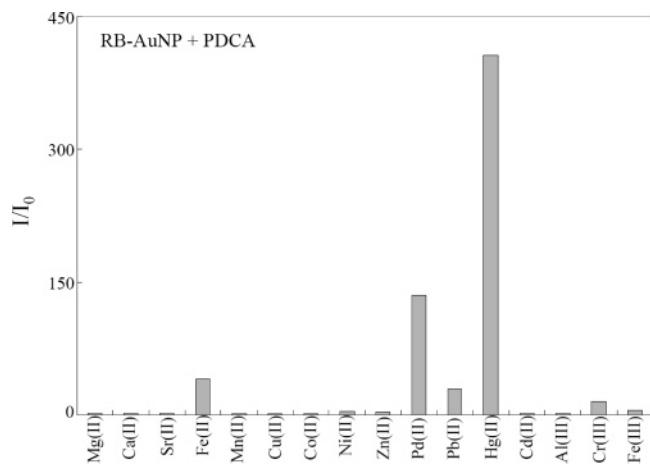


**Figure 4.** Enhance ratios ( $I/I_0$ ) of the fluorescence intensity (575 nm) of 1.0 mM PDCA-assisted RB-AuNP in 5 mM sodium tetraborate solutions (pH 9.0) upon the addition of 100  $\mu\text{M}$  metal ions. Other conditions were the same as those described for Figure 1.

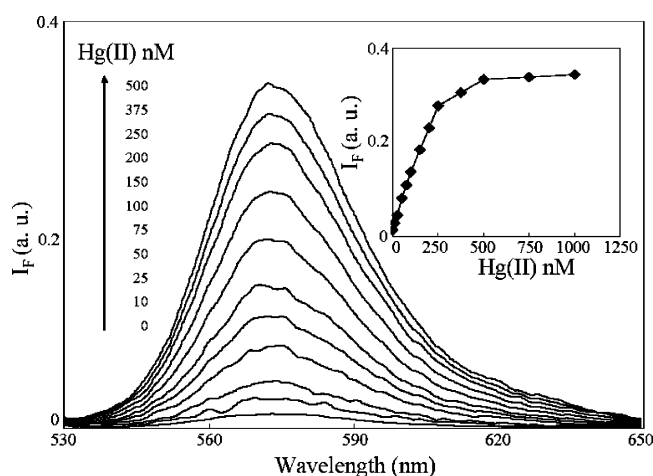


**Figure 5.** Fluorescence response of RB-AuNP-MPA (0.6 nM) upon addition of Hg(II) ions (0, 10, 25, 50, 75, 100, 150, 200, 250, 375, and 500 nM). Inset: Fluorescence intensity (575 nm) versus Hg(II) concentration. Other conditions were the same as those described for Figure 1.

To test the practical applicability of using the RB-AuNP-MPA system as a Hg(II)-selective fluorescence nanosensor, we performed a series of competitive experiments. After adding Hg(II) (10  $\mu\text{M}$ ) and background interference metal ions (100  $\mu\text{M}$ ) to a mixture of RB-AuNP-MPA and PDCA (1.0 mM), we did not observe any significant interference of the detection of Hg(II) ions (Figure S2, Supporting Information). In addition, the enhancement in fluorescence intensity resulting from the addition of Hg(II) was not influenced by the subsequent addition of other metal ions (data not shown).

**Sensitivity and Application.** As indicated in Figure 5, the intensity of the fluorescence emission of RB-AuNP-MPA was sensitive to Hg(II) ions and increased as the concentration of Hg(II) increased. A linear correlation existed between the emission intensity and the concentration of Hg(II) over the range 15–250 nM ( $R^2 = 0.98$ ). The LOD at an S/N ratio of 3 for Hg(II) was 10 nM (2.0 ppb), which is the maximum level of mercury in drinking water permitted by the United States Environmental Protection Agency (EPA). This approach provides a sensitivity 2 orders of magnitude lower than that of the reported data by a chelation/

**Table 1. Determination of the Concentrations of Hg(II) in Three Different Types of Alkaline Manganese Batteries by PDCA-Assisted RB-AuNP-MPA and ICPMS**

battery	RB-AuNP-MPA, mean $\pm$ SD (mg/g, $n = 5$ )	ICPMS, mean $\pm$ SD (mg/g, $n = 5$ )	$F$ -test between the two methods <sup>a</sup>
a	0.97 $\pm$ 0.09	1.10 $\pm$ 0.10	1.2
b	2.28 $\pm$ 0.12	2.46 $\pm$ 0.15	1.6
c	1.58 $\pm$ 0.06	1.65 $\pm$ 0.07	1.4

<sup>a</sup> The  $F$ -test value is 6.39 at a 95% confidence level.

aggregation-mediated colorimetric and modulation of photoluminescent quenching AuNP-based heavy metal ion sensor.<sup>8a,b,e</sup>

This new Hg(II)-based nanosensor also exhibited great potential for the analysis of Hg(II) in environmental samples. A water sample from a pond on our campus was filtered through a 0.2  $\mu\text{m}$  membrane and then subjected to ICPMS analysis; the concentration of Hg(II) was determined to be 0.6 ppb. This result agrees with our observation of almost no increase in fluorescence after addition of 0.6 mL of the pond water to 0.4 mL of 5 mM sodium tetraborate solution containing 0.6 nM RB-AuNP-MPA (data not shown). To determine the concentration of Hg(II) in the sample, we applied a standard addition method. A linear correlation existed between the emission intensity and the concentration of Hg(II) ions spiked in the pond water over the range 15–250 nM ( $R^2 = 0.96$ ; Figure S3, Supporting Information). The recoveries of these measurements were 90–95%. The LOD at an S/N ratio of 3 for Hg(II) was also 10 nM (2.0 ppb) in the complicated pond water matrix. Our results suggest that this probe will be useful for detecting environmentally relevant concentrations of Hg(II). To further demonstrate the feasibility of this approach, the concentrations of Hg(II) in batteries were determined. The mercury batteries tested have a mercuric oxide cathode that usually contains 20–50% mercury by weight. Table 1 lists the concentrations of Hg(II) in three different types of batteries that were determined by this approach and ICPMS. On the basis of the  $F$ -test, the results from our present approach are in good agreement with those from ICPMS.

## CONCLUSIONS

We have demonstrated a new homogeneous assay for detecting Hg(II) ions; it is based on modulation of the photoluminescence quenching efficiency of RB and AuNPs in the presence of Hg(II) ions. The large turn-on fluorescence enhancement (400-fold) for sensing Hg(II) in aqueous solution results from the very low fluorescence of RB molecules adsorbed onto AuNP surfaces. We improved the selectivity of the probe further by modifying the AuNP surfaces with thiol ligands (MPA, MSA, and HCys) and adding PDAC to the sample solutions. Under the optimum conditions, the selectivity of this system for Hg(II) over other metal ions in aqueous solutions was remarkably high, and its LOD was 2.0 ppb. In addition, the present approach provides the advantages of rapidity (<10 min), simplicity, and low cost. We believe that this approach may serve as a foundation for the preparation of practical nanosensors for the rapid determination of Hg(II) concentrations in aqueous biological and environmental samples.

## ACKNOWLEDGMENT

This study was supported by the National Science Council of Taiwan under Contract NSC 95-2113-002-026-MY3.

## SUPPORTING INFORMATION AVAILABLE

Enhanced ratios ( $I/I_0$ ) of the fluorescence intensity of PDCA-assisted RB–AuNP–MSA and RB–AuNP–HCys systems (Figure S1), enhanced ratios ( $I/I_0$ ) of the fluorescence intensity of RB–AuNP–MPA solutions containing PDCA upon the addition of Hg-

(II) in the presence of background metal ions (Figure S2), and fluorescence response of RB–AuNP–MPA upon addition of Hg-(II) ions to a matrix of pond water (Figure S3). This material is available free of charge via the Internet at <http://pubs.acs.org>.

Received for review August 10, 2006. Accepted October 4, 2006.

AC061487I